Adsorption 2, 279–286 (1996)

Equilibrium Adsorption Data from Temperature-Programmed Desorption Experiments

FRANK FOETH, JOSÉ MUGGE, RICK VAN DER VAART, HANS BOSCH AND TOM REITH
Faculty of Chemical Technology, University of Twente, P.O. Box 217, 7500 AE Enschede, The Netherlands

Received January 3, 1996; Revised May 21, 1996; Accepted May 29, 1996

Abstract. This work describes a novel method that enables the calculation of a series of adsorption isotherms basically from a single Temperature-Programmed Desorption (TPD) experiment. The basic idea is to saturate an adsorbent packed in a fixed bed at a certain feed concentration and temperature and to subsequently increase its temperature linearly with time, while maintaining a constant feed concentration.

We measured TPD response curves for carbon dioxide on activated carbon at different heating rates for various combinations of feed concentration, molar flow rate and particle size. Response curves from an axially dispersed plug flow model were fitted to experimental data by adjustment of the Langmuir parameters. Adsorption isotherms calculated with these fitted parameters are in good agreement with adsorption data obtained by other methods over the full temperature range.

The influence of heating rate on intraparticle mass transfer resistance is discussed.

Keywords: mathematical models, experimental data, measurement method, thermal desorption

Introduction

In fixed-bed adsorbers considerable temperature gradients may develop during dynamic sorption processes, such as (rapid) pressure swing adsorption. The proper design of such adsorbers require adsorption data within a broad temperature range. Measurements of adsorption isotherms by usual gravimetric or volumetric equilibrium methods to measure the adsorption isotherms within the required temperature range are very time consuming.

Under certain experimental conditions equilibrium adsorption data can be obtained faster from dynamic experiments, thus reducing the number of experiments. Bosch and Peppelenbos (1977) showed that BET surface areas calculated from a continuous pressure increase at a constant adsorbate feed rate agree excellent with results from equilibrium methods. Foeth et al. (1994) calculated equilibrium adsorption data from breakthrough curves, taking into account the change in both velocity and pressure during breakthrough if necessary (Foeth et al., 1996).

A similar development has taken place in measuring activation energies. The usual method is to measure at various temperatures either initial reaction rates or rate constants in steady state experiments. Unlike these constant temperature methods, it is possible to determine the Arrhenius constants of first order reactions from only a single run of rate measurements using a linear rise in temperature with time instead of multiple runs at constant temperature each. This has been shown, among many others, by Wold and Ahlberg (1970), Marsh and Taylor (1977), and Amasaki et al. (1989). The activation energies of more complex reactions can be evaluated also from a single temperature-programmed run, provided the mechanism of the reaction is known, e.g., Bosch (1989).

Combining these approaches, a dynamic method can be envisaged that enables the calculation of a series of adsorption isotherms from a limited number of experiments. The basic idea of this novel method is to saturate an adsorbent at a certain feed concentration and temperature and subsequently to create a linear rise in temperature with time, while maintaining a constant

feed concentration. From the measured change in exit concentration, the amounts adsorbed can be calculated over the full temperature range. Runs at a few different feed concentrations would then allow the calculation of a series of adsorption isotherms in the range of exit concentrations measured.

The future objective is to develop an efficient method to measure multicomponent adsorption equilibria. The goal of this work, while limiting ourselves to single component desorption, is to show that equilibrium adsorption data can be extracted from this Temperature-Programmed Desorption Method.

Experimental

We measured TPD response curves for the adsorption of CO_2 from CO_2/He mixtures on a fixed bed of activated carbon (RB1, courtesy Norit) at 313–353 K, see Table 1. The carbon was characterized by static gravimetric adsorption (IGA, Hiden Analytical) and volumetric adsorption (Sorptomatic, 1900; Carlo Erba) of CO_2 at 313.1, 323.1 and 349.3 K.

To ensure a flat temperature profile over the sample, TPD runs were carried out in a copper reactor (19 cylindrical holes each with length $L = 4.2$ cm and $ID = 3$ mm) immersed in a water bath. Helium with a purity of 99.999% (HoekLoos) and carbon dioxide with a purity of 99.996% (HoekLoos) were used without further purification. The composition of the feed was controlled by two mass flow controllers. The exit concentration was monitored by means of a thermal conductivity detector (TCD). During the experiment the exit molar flow changes. The TCD was calibrated accordingly with a constant flow of helium, adding appropriate flows of carbon dioxide to cover the experimental range of mole fractions from 0.1 to 0.3 at the column exit. The validity of the isotherms to be calculated is limited by this range.

Prior to each TPD run the following procedure was performed:

1. *In situ* conditioning of the sample in inert gas at initial temperature T_0.
2. Addition of the adsorbable component and its subsequent isothermal breakthrough.

These breakthrough curves were used to calculate the initially adsorbed quantity (Amasaki et al., 1989; Bosch and Pepplenbos, 1977), q_0, at the start of each TPD experiment.

During an actual TPD run, a linear temperature increase was enforced by appropriate programming of the water bath. The influence of heating rate, molar flow rate and particle size were investigated at two different feed compositions; see Table 1.

Models

We developed an axially dispersed plug flow model to calculate the change in exit concentration as a function of the temperature at the experimental conditions given in Table 1. The model was set up for a binary mixture with one adsorbable component, having the following assumptions:

- Radial concentration gradients are absent,

Table 1. Experimental conditions.

Sample weight [g]	Particle size [mm]	Flow rate [μmol/s]	Heating rate [mK/s]	Pe_0	Symbol in Figs. 1 and 3
$y_f = 0.200$					
2.573	0.21–0.30	13.9	46.0	6	■
2.573	0.21–0.30	13.9	18.2	6	□
2.573	0.21–0.30	27.8	47.0	12	⊠
2.573	0.21–0.30	27.8	18.5	12	⊠
$y_f = 0.100$					
2.573	0.21–0.30	13.9	18.5	6	○
2.874	0.105–0.150	13.9	41.3	8	▲
2.874	0.105–0.150	13.9	18.7	8	△
2.573	0.21–0.30	13.9	42.5	6	
2.573	0.21–0.30	27.8	44.7	12	

Pe_0 = coefficient of axial dispersion calculated at the initial conditions with Eq. (6).

- Both radial and axial temperature gradients are absent,
- Total pressure is constant,
- Local adsorption equilibrium between the solid and the surrounding gas phase is established, and
- Adsorption equilibria, within the experimental range of partial pressure and temperature, are described by a Langmuir type equation:

$$q = \frac{q_m b_0 e^{-\Delta H_a/RT} y P}{1 + b_0 e^{-\Delta H_a/RT} y P} \tag{1}$$

q_m, b_0 and ΔH_a are the Langmuir parameters to be determined by fitting the model to the experimental response curves. The Langmuir model was used because of its simplicity while it describes not only concentration changes but also the influence of temperature on the amount adsorbed.

Based on the same assumptions we also used a tanks-in-series model, describing the transient behaviour of the actual reactor as that of a few ideally stirred tank reactors in series, for two reasons:

- To provide reasonable estimates of the Langmuir parameters to be fitted in the former method;
- To check the results of the dispersed plug flow model at small concentration changes.

Tanks-In-Series Model

The accumulation of an adsorbate in a single tank reactor, Wr_a, neglecting its accumulation in the gas phase, follows from the mole balances for both components:

$$Wr_a = \frac{y_f - y_e}{1 - y_e}\phi_f \tag{2}$$

with ϕ = molar flow rate and y_f, y_e = mole fraction at inlet and exit, respectively. A positive value of the adsorption rate per unit weight r_a indicates adsorption, a negative value indicates desorption. For Langmuir adsorption the change in r_a with time t depends on both concentration and temperature T:

$$\begin{aligned} r_a &= \left.\frac{\partial \bar{q}}{\partial y}\right|_T \frac{dy}{dt} + \left.\frac{\partial \bar{q}}{\partial T}\right|_y \frac{dT}{dt} \\ &= \frac{q_m bP}{(1+ybP)^2}\frac{dy}{dt} + \frac{q_m ybP}{(1+ybP)^2}\frac{\Delta H_a}{RT^2}\frac{dT}{dt} \end{aligned} \tag{3}$$

Elimination of r_a from Eqs. (2) and (3), introducing a constant heating rate $\beta = \frac{dT}{dt}$, yields the following expression for the change of exit mole fraction y_e of each tank with a change of ΔT in temperature:

$$\frac{\Delta y_e}{y_e} = \left[-\frac{\Delta H_a}{RT} + \frac{T}{\beta}\frac{\phi_f}{W q_m f(y_e)}\frac{y_f - y_e}{1 - y_e}\right]\frac{\Delta T}{T} \tag{4}$$

where $f(y_e) = (1 - q/q_m)\cdot q/q_m$. The number of tanks in series required to account for the actual axial dispersion depends on the Péclet number and is calculated with Eq. (10). Equation (3) is subsequently applied to each of these tanks, noting that the inlet mole fraction y_f of a tank equals the outlet mole fraction y_e of the previous one.

Axially Dispersed Plug Flow Model

A more accurate calculation of the concentration change with temperature in a TPD experiment is obtained, analogously to an approach suggested by Huang and Schwarz (1986), starting from a differential mole balance equation:

$$\frac{\partial y c_t}{\partial t} + \frac{W}{\varepsilon A L} r_a = -\frac{1}{\varepsilon A}\frac{\partial y\phi}{\partial z} + \frac{\partial}{\partial z}\left(D_T c_t \frac{\partial y}{\partial z}\right) \tag{5}$$

where the adsorption rate r_a is given by Eq. (3). In modelling temperature-programmed processes, it is convenient to use temperature as the independent parameter with $T = T_0 + \beta t$. The coefficient of axial dispersion D_T appears to be slightly lower than the molecular diffusion, as will be shown in the next section, therefore we put $D_T = D_0(T/T_0)^{1.75}$. Here the axial Péclet number Pe is a function of temperature:

$$\mathrm{Pe} = \frac{L}{D_0 \Theta^{1.75}}\frac{\phi_f}{\varepsilon_b A P/RT_0} \tag{6}$$

where $\Theta = T/T_0$. Introducing a dimensionless distance $Z = z/L$ and a dimensionless molar flow rate $\Phi = \phi/\phi_f$, Eq. (5) transforms into the following PDE:

$$\begin{aligned} \tau_{\mathrm{rh}}\left[1 + \nu_{\mathrm{ag}}\frac{f(y)\Theta}{y}\right]\frac{\partial y}{\partial \Theta} &= -\tau_{\mathrm{rh}}\nu_{\mathrm{ag}}\frac{f(y)}{\Theta}\frac{\Delta H_a}{RT_0} + \frac{\tau_{\mathrm{rh}}}{\Theta}y \\ &\quad - \Theta\frac{\partial y\Phi}{\partial Z} + \frac{1}{\mathrm{Pe}}\frac{\partial^2 y}{\partial Z^2} \end{aligned} \tag{7}$$

with ν_{ag} is equal to the ratio of adsorbent capacity and holdup in the gas phase and τ_{rh} is equal to the ratio of mean residence time of inert and time constant of heating; $f(y)$ is defined in Eq. (4). Equation (7) describes

the change in concentration of the adsorbate as a function of position and temperature. A similar equation exists for the non-adsorbing component. Taking the sum of the latter equation and Eq. (7) yields:

$$\nu_{ag}\frac{f(y)\Theta}{y}\frac{\partial y}{\partial \Theta} = -\nu_{ag}\frac{f(y)}{\Theta}\frac{\Delta H_a}{RT_0} + \frac{1}{\Theta} - \frac{\Theta}{\tau_{rh}}\frac{\partial \Phi}{\partial Z} \tag{8}$$

The initial conditions are:

$$\Theta = 1 \quad 0 \le Z \le 1 \quad \Phi = 1 \quad y = y_f \tag{9a}$$

and the boundary conditions are:

$$\Theta \ge 1 \quad Z = 0 \quad \Phi = 1 \quad \left.\frac{\partial y}{\partial Z}\right|_{Z=0} = \mathrm{Pe}\Theta(y - y_f) \tag{9b}$$

$$\Theta \ge 1 \quad Z = 1 \quad \left.\frac{\partial y}{\partial Z}\right|_{Z=1} = 0 \tag{9c}$$

This system of PDEs was solved by the numerical method of lines. First, the system of PDEs was converted to a system of ODEs by inserting five point finite difference approximations of the derivatives in space from DSS/2 (Schiesser, 1991). Second, the resulting system of ODEs was implicitly solved in time by the integrator LSODI (Hindmarsh, 1983).

Results

Experimental TPD Response Curves

Figure 1 shows the reduced exit mole fraction y_e/y_f as a function of temperature at the various combinations of feed composition, flow rate, heating rate and particle size given in Table 1. It should be noted that the experimental results, for clarity given as symbols in Fig. 1, have been monitored continuously. All experimental TPD response curves have the same characteristic form:

- Initially an almost linear increase due to desorption, followed by
- A maximum where the desorption rate is balanced by the net discharge from the column as can be seen from the LHS in Eq. (4) and, finally,
- A slow decrease; the curve eventually approaches the initial feed composition.

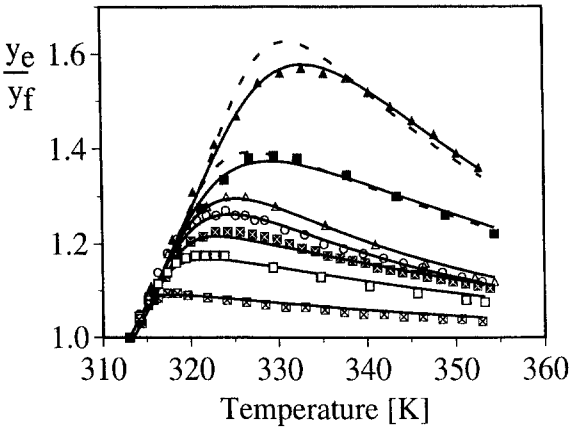

Figure 1. TPD response curves. Symbols: experimental results (see Table 1 for the meaning of the symbols) solid lines: fitted axially dispersed plug flow; dashed lines: tanks-in-series.

Model Calculations

The Péclet numbers Pe_0, defined at the initial conditions, calculated with Eq. (6) are given in Table 1. For an estimate of the coefficient of axial dispersion we used a relation discussed by Wicke (1973) for particles with $d_p < 2.5$ mm (Langer, 1978) resulting in an average value of $D_0 = 4.3\ 10^{-5}$ m^2/s, which is approximately 10% lower than the molecular diffusivity. In the tanks-in-series model the number of tanks N was calculated from:

$$N = 1 + \mathrm{Pe}_0/2 \tag{10}$$

Response curves calculated with both models were the same for reduced changes in exit mole fraction less then 20%. At larger concentration differences the tanks-in-series model predicts a higher maximum in the response curve; two examples are shown in Fig. 1.

Curve Fitting

The amount adsorbed, q_0, was determined from the initial breaktrough curve. With this value the adsorption constant b_0 was eliminated from Eq. (1) using:

$$b_0 = \frac{\exp(\Delta H_a/RT_0)}{y_f P(q_m/q_0 - 1)} \tag{11}$$

We adjusted the remaining Langmuir parameters, ΔH_a and q_m, to fit the experimental response curves. ΔH_a

was estimated from the initial slope using Eq. (3); q_m was estimated from the remainder of the response curve. These estimates were used as initial guesses in a least squares optimization simultaneously for all experiments shown in Fig. 1. The results from model calculations are in good agreement with the experimental results for $q_m = 1.78$ mol/kg, $\Delta H_a = -28.3$ kJ/mol and, from Eq. (11), $b_0 = 4.92\ 10^{-10}$ m^2/N. Although one experiment is sufficient to obtain estimates for the Langmuir parameters, all experiments labelled in Table 1 were fitted simultaneously to increase accuracy.

With $y_f = 0.100$, however, only the combination of larger particles and higher heating rate could not be fitted simultaneously (experiments shown in Table 1 without symbols). The initial slope of the response curves in these experiments was identical with those of all other experiments. A separate optimization for the latter two experiments resulted in the same ΔH_a and a 30% lower value of q_m. Reasons for this will be discussed in the Discussion section.

Adsorption Isotherms

Figure 2 shows adsorption data measured by volumetric and gravimetric equilibrium techniques, as well as adsorption data calculated from breakthrough curves (Amasaki et al., 1989; Bosch and Pepplenbos, 1977). TPD adsorption data, calculated at the indicated temperatures from the fitted values of the Langmuir parameters and shown as solid lines in Fig. 2, are in good agreement with the adsorption data obtained from the other methods.

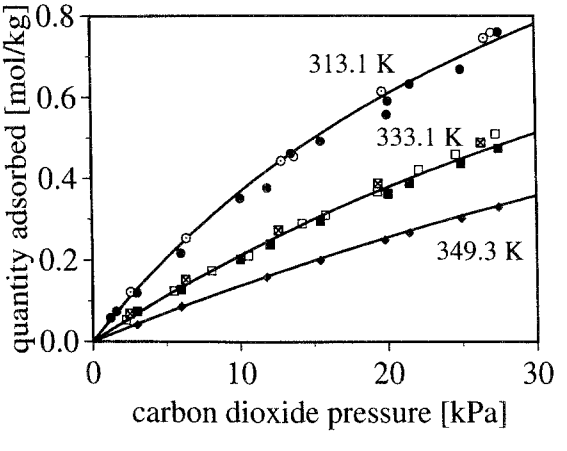

Figure 2. Isotherms calculated from TPD compared to adsorption data from other methods. Solid lines TPD; ○□ volumetric; ●■♦ gravimetric; ⊙⊠ breakthrough.

Discussion

Unlike usual TPD techniques, we used TPD response curves to determine adsorption isotherms. Hence the experimental conditions in both types of TPD techniques differ substantially. In the former conditions are optimized to characterize adsorption sites, see e.g., (Cvetanovic and Amenomiya, 1967) Rajadurai, 1994) or to obtain kinetic parameters of (surface) chemical reactions, see e.g., Cvetanovic and Amenomiya (1972), Hinrichsen (1994). Typical heating rates applied to characterize catalysts range from 0.3 to 1 K/s (Falconer and Schwarz, 1983). On the other hand, the heating rates used in this work are much lower because local adsorption equilibrium had to be ensured. No attempt was made to minimize axial dispersion or readsorption effects; these were taken into account in the models we used. Moreover, a constant feed composition was maintained during the desorption because physisorption was investigated. Hence the purpose, the conditions and the procedure of the present TPD method differ widely from common TPD techniques.

To obtain experimental evidence for the assumption of local equilibrium adsorption, we carried out TPD experiments with different combinations of heating rate, particle size, flow rate and feed concentration, see Table 1. The same set of Langmuir parameters has been found for the combination of process conditions used in the experiments shown in Fig. 1. Figure 3 shows an error plot comparing experimental reference data and TPS adsorption data calculated at the relevant conditions. All data appear to be evenly spread around the average value; the standard deviation amounting to 0.038. The experimental data have been obtained from several laboratories by different techniques on different samples from the same batch. Taking this into consideration, it is concluded that fitted experiments and model calculations agree well and that mass transfer resistance in the particles could be neglected in all labelled experiments.

The assumption of negligible intraparticle concentration gradients is not satisfied under the experimental conditions of the last two experiments given in Table 1, because for these two experiments the calculated value for q_m is 30% lower than the equilibrium value. However, all experiments—including the last two experiments—presented satisfy the criterium for

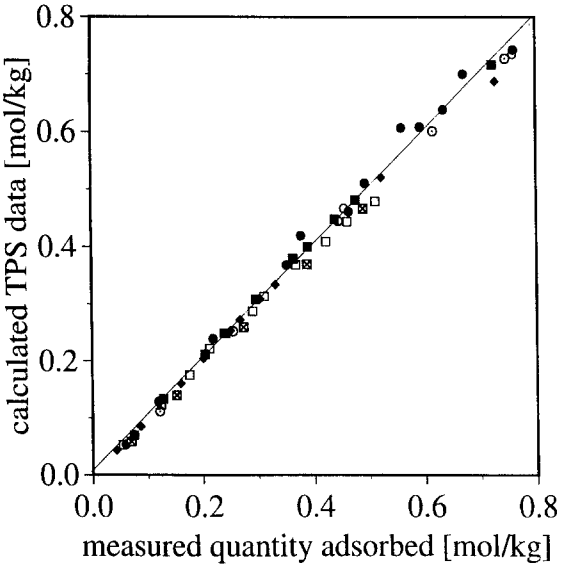

Figure 3. Comparison of calculated TPD adsorption data and experimental reference adsorption data (see Table 1 for the meaning of the symbols).

negligable intraparticle concentration gradients, as developed by Demmin and Gorte (1984). We note that the latter two experiments have in common the following experimental conditions: larger particle size, higher heating rate and lower feed concentration. Heating rate and feed concentration are not taken into account in the Demmin and Gorte criterium.

To analyze this discrepancy, firstly we discuss the location of the major temperature gradient. Within a porous particle the effect of temperature distribution is usually much less important than internal diffusion limitation (Akehata et al., 1961). Considering film resistance, we estimated thermal Biot numbers $Bi_h = hd_p/6\lambda$, the ratio of thermal resistance of a spherical particle to that of the film using correlations for heat transfer coefficients in packed beds at low Re numbers (Littman et al., 1968). We found $Bi_h < 2.10^{-4}$, indicating that temperature gradients, if any, are entirely in the film around the particles.

Secondly, we use the following equation (Mears, 1971) to estimate the deviation $\Delta_r = |r_a - r_{obs}|$ from the sorption rate r_a at the temperature of the bulk gas T_b adjacent to a particle due to film resistance:

$$\left|\frac{\Delta r}{r_a}\right| = \left|\frac{-r_{obs}\rho_p d_p \Delta H_a}{6hT_b}\frac{E_d}{RT_b}\right| \qquad (12)$$

where E_d = activation energy for desorption and h = gas-solid heat transfer coefficient. With Eq. (2) the observed net rate of desorption per unit particle volume $r_{obs} \cdot \rho_p$ can be calculated from the experimental response curves given in Fig. 2. With a maximum value of $r_{obs} \cdot \rho_p$ observed in this work of 0.6 mol/m^3 s^1 and as $E_d \approx |\Delta H_a|$ in case of physisorption, it follows that in all experiments reported here the deviation from r_a due to interphase heat transport limitation is less than 1%. We conclude that in this work temperature gradients are negligable.

Analogously, using a Chilton-Colburn J_D factor relation for low Reynolds numbers (Carberry, 1976), we found for the mass Biot number $Bi_m = k_{gs}d_p/6D_e > 6$. We conclude that the major concentration gradient will be an intraparticle one.

Finally, we examine the parameters that influence mass transfer limitation in an isothermal particle. The assumption of local adsorption equilibrium implies the lumped mass transfer coefficoent k_{gs} in a simple linear driving force model:

$$r_a = \frac{d\bar{q}}{dt} = k_{gs}(q^* - \bar{q}) \qquad (13)$$

is sufficiently large to ensure $q^* \approx \bar{q}$. Glueckauf and Coates (1947) showed that in the isothermal case at low concentrations (linear isotherm), neglecting film and intracrystalline diffusion

$$k_{gs} = \frac{60\varepsilon_p D_e}{K(y)d_p^2} \qquad (14)$$

On the other hand, inspection of Eq. (3) shows that, at least initially, r_a is proportional to the heating rate $\beta = dT/dt$. Hence, in TPD systems the mass transfer resistance for pore diffusion is, initially, proportional to $\frac{K(y)d_p^2}{60\varepsilon_p D_e}\frac{\beta}{T_0}$.

The highest mass transfer resistance is achieved at the highest heating rate with the largest particles at the lowest concentration (larger slope of the isotherm). Under the experimental conditions of the last two experiments mentioned in Table 1, the intraparticle mass transfer resistance is 2 to 10 times larger than for the other experiments, labeled with a symbol. The higher intraparticle mass transfer resistance probably results in noticable intraparticle concentration gradients in case of these two experiments.

Our future plans include experiments to investigate in more detail the parameters influencing heat and mass transfer in TPD measurements involving multicomponent physisorption, in particular by comparing results from experiments with particles of different sizes

at both increasing and decreasing temperature. Meanwhile we feel that we developed a rapid and convenient method to determine heats of adsorption and monolayer capacities, from which any adsorption isotherm within the experimental temperature and concentration range can be calculated.

Conclusion

Temperature-Programmed Desorption provides a powerful method to obtain all the adsorption data required for design purposes in a certain temperature range from a very limited number of measurements with standard laboratory equipment.

Nomenclature

A : cross sectional area, m^2
A_p : particle surface area, m^2/kg
b : adsorption constant in Langmuir equation, m^2/N
b_0 : pre-exponantial factor in $b = b_0 \exp(-\Delta H_a/RT)$, m^2/N
Bi : ratio of particle resistance to film resistance, $Bi_m = k_{gs}d_p/6D_e$; $Bi_h = hd_p/6\lambda$
c_t : adsorbate concentration (subscript t = total concentration, b = bulk), mol/m^3
d_p : particle diameter, m
D_T : coefficient of axial dispersion (subscript 0 at temperature T_0), m^2/s
D_e : effective intraparticle diffusivity, m^2/s
E_d : activation energy of desorption, J/mol
$f(y_e)$: $(1 - q/q_m)q/q_m$, Eqs. (4), (7) and (8)
h : gas-solid heat transfer coefficient, W/m^2 K
ΔH_a : heat of adsorption, J/mol
J_D : Chilton-Colburn J_D factor for mass transfer,
k_{gs} : mass transfer coefficient, 1/s
$K(y)$: slope of adsorption isotherm,
L : column length, m
M : molecular weight of adsorbate, kg/mol
N : number of ideal stirred tank reactors
P : total pressure, N/m^2
Pe_0 : Péclet number defined at inlet at initial temperature $= \frac{L}{D_0}\frac{\phi_f}{\varepsilon AP/RT_0}$,
q : amount CO_2 adsorbed per unit weight adsorbent (subscript m = monolayer capacity, superscript $*$ = amount adsorbed at gas phase concentration just outside particle) mol/kg
q_m : monolayer capacity, mol/kg
r_a : adsorption rate per unit weight adsorbent at the temperature T_b of the gas film surrounding the particle ($r_a < 0$ means desorption), mol/kg s
r_{obs} : observed adsorption rate per unit weight adsorbent, mol/kg s
R : gas constant, J/mol K
t : time, s
T : temperature (T_0 at time $t = 0$, bulk gas temperature T_b), K
W : weight of adsorbent, kg
y : mole fraction CO_2 (subscript f = feed, e = exit),
z : distance, m
Z : z/L,
β : heating rate, K/s
ε : fractional void space (subscript b = bed, t = total, p = particle),
ϕ_f : molar feed flow, mol/s
ϕ_m : molar flow, mol/s
F : $\phi - m/\phi_f$,
λ : heat conductivity, W/m K
ν_{ag} : adsorbent capacity/holdup in gas phase $= \frac{Wq_m}{\varepsilon_t ALP/RT_0}$,
ρ_p : particle density, kg/m^3
τ_{rh} : ratio of mean residence time of inert and heating rate $= \frac{\varepsilon_t ALP/RT_0}{\phi_f}\frac{\beta}{T_0}$,
Θ : dimensionless temperature T/T_0

Acknowledgment

The financial support of SON is gratefully acknowledged. We wish to express our gratitude to Dr. Rob de Lange (University of Twente) and Mr. Jan Loos (University of Delft) for the volumetric adsorption measurements. We also wish to thank the student Mr. Wouter van Marle for performing the TPD experiments.

References

Akehata, T., S. Namkoong, H. Kubota, and M. Shindo, "The Effect of Intraparticle Temperature Distribution on the Catalytic Effectiveness Factor of a Porous Catalyst," *Can. J. Chem. Eng.*, June, 127–129 (1961).

Amasaki, I., M. Nakada, and M. Hirota, "Determination of the Arrhenius Parameters Using a Linear Programmed Temperature Elevation System," *Nippon Kagaku Kaishi*, **10**, 1672–1676 (1989).

Bosch, H. and A. Peppelenbos, "Automatic and Low-Cost Determination of BET Surface Areas," *J. Phys. E: Sci. Instrum.*, **10**, 605–608 (1977).

Bosch, H. and P.J. Sinot, "Activation Energies of the Reduction of Bulk and Supported Vanadium Pentoxide," *J. Chem. Soc., Faraday Trans. 1*, **85**, 1425–1437 (1989).

Carberry, J.J., *Chemical and Catalytic Reaction Engineering*, p. 494, McGraw-Hill (1976).

Cvetanovic, R.J. and Y. Amenomiya, "Application of a Temperature-Programmed Desorption Technique to Catalyst Study," *Adv. Catal.*, **17**, 103–125 (1967).

Cvetanovic, R.J. and Y. Amenomiya, "A Temperature-Programmed Desorption Technique for Investigation of Practical Catalysts," *Catal. Rev.*, **6**, 21–48 (1972).

Demmin, R.A. and R.J. Gorte, "Design Parameters for Temperature-Programmed Desorption from a Packed Bed," *J. Catal.*, **90**, 32–39 (1984).

Falconer, J.L. and J.A. Schwarz, "Temperature-Programmed Desorption and Reaction: Applications to Supported Catalysts," *Catalytic Reviews, Science and Engineering*, **25**, 141–227 (1983).

Foeth, F., M. Andersson, H. Bosch, G. Aly, and T. Reith, "Separation of Dilute CO_2—CH_4 Mixtures by Adsorption on Activated Carbon," *Sep. Sci. Technol.*, **29**, 93–118 (1994).

Foeth, F., H. Bosch, A. Sjöstrand, G. Aly, and T. Reith, "Equilibrium Adsorption Data from Breakthrough Curves with Variable Velocity and Pressure," *Sep. Sci. Technol.*, **31**, 21–38 (1996).

Glueckauf, E. and J.I. Coates, "Theory of Chromatography. Part IV: The Influence of Incomplete Equilibrium on the Front Boundary of Chromatograms and on the Effectiveness of Separation," *J. Chem. Soc.*, 1315–1321 (1947).

Hindmarsh, A.C., Ed. ODEPACK, A Systematized Collection of ODE solvers, *IMACS Transactions on Scientific Computation*, North-Holland Publishing Company, Amsterdam (1983).

Hinrichsen, O., F. Rosowski, and M. Muhler, "Microkinetic Modelling of TPD of Nitrogen from Industrial Synthesis Catalyst," *Chem.-Ing.-Tech.*, **66**, 1375–1378 (1994).

Huang, Y.-J. and J.A. Schwarz, "Influence of the Temperature-Ramp on Mass Transfer Effects During Temperature-Programmed Desorption from Porous Catalysts," *J. Catal.*, **99**, 249–251 (1986).

Langer, G., A. Roethe, K.-P. Roethe, and D. Gelbin, "Heat and Mass Transfer in Packed Beds—III: Axial Mass Dispersion," *Int. J. Heat Mass Transfer*, **21**, 751–759 (1978).

Littman, H., R.G. Barile, and A.H. Pulsifer, "Gas-Particle Heat Transfer Coefficients in Packed Beds at Low Reynolds Numbers," *Ind. Eng. Chem. Fundam.*, **7**, 554–561 (1968).

Marsh, H. and D.W. Taylor, "Kinetics of the Carbon-Carbon Dioxide Reaction Under a Continuous and Linear Increase in Temperature," *Carbon*, **15**, 265–266 (1977).

Mears, D.E., "Diagnostic Criteria for Heat Transport Limitations in Fixed Bed Reactors," *J. Catal.*, **20**, 127–131 (1971).

Rajadurai, S., "Pathways for Carboxylic Acid Decomposition on Transition Metal Oxides," *Catalytic Reviews, Science and Engineering*, **36**, 388–389 (1994).

Schiesser, W.E., *The Numerical Method of Lines: Integration of Partial Differential Equations*, Academic Press Inc., San Diego (1991).

Wicke, E., "Bedeutung Der Molekularen Diffusion für chromatographische Verfahren," *Ber. Bunsenges.*, **77**, 160–171 (1973).

Wold, S. and P. Ahlberg, "Evaluation of Activation Parameters for a First Order Reaction from One Kinetic Experiment. Theory, Numerical Methods and Computer Program," *Acta Chem. Scan.*, **24**, 618–632 (1970).